DALTON
FULL PAPER

Syntheses, crystal structures and magnetic properties of one- and two-dimensional pap-containing copper(II) complexes (pap = pyrazino[2,3-*f*][4,7]phenanthroline)

Hilde Grove,[a] Jorunn Sletten,*[a] Miguel Julve,[b] Francesc Lloret[b] and Juan Cano[b]

[a] *Department of Chemistry, University of Bergen, Allégaten 41, N-5007 Bergen, Norway*
[b] *Department of Inorganic Chemistry, Faculty of Chemistry, University of Valencia, Dr. Moliner 50, 46100 Burjassot (Valencia), Spain*

Received 3rd October 2000, Accepted 5th December 2000
First published as an Advance Article on the web 15th January 2001

Three polynuclear complexes containing copper(II) and pyrazino[2,3-*f*][4,7]phenanthroline (pap) as the basic building blocks have been prepared $[Cu_2(pap)(H_2O)_2(NO_3)_3]_n[NO_3]_n$ **1**, $[Cu_4(pap)_4Cl_7]_nCl_n\cdot 15nH_2O$ **2**, and $[Cu_4(pap)_4(H_2O)_4(C_4O_4)_2]_n[C_4O_4]_n[NO_3]_{2n}\cdot 12nH_2O$ **3**, and their crystal structures and variable-temperature magnetic susceptibilities determined. Compound **1** is a single stranded zigzag chain where pap and nitrate alternate as bridges between the copper atoms. The copper coordination geometry is to a first approximation distorted square pyramidal, but with an additional semi-coordinated oxygen from non-bridging nitrate groups. The bridging nitrate coordinates in the apical position to both copper atoms. In **2** the basic structural unit is a cyclic, tetranuclear entity where copper atoms are bridged by pap. Two different pap bridges are present, one through only equatorial positions, the other coordinating equatorially and axially. These tetranuclear units are linked, through diagonally opposite corners, into chains by single atom chloro-bridges. The copper coordination geometry is distorted elongated octahedral. In **3** a tetranuclear building block, with structural characteristics similar to those found in **2**, is present, but in this case coordinated squarate (3,4-dihydroxycyclobut-3-en-1,2-dionate) links these units into sheets. Neighbouring sheets are firmly connected by hydrogen bonds through uncoordinated squarate and water into a three-dimensional supramolecular structure featuring channels running normal to the sheets. The Cu · · · Cu separations across bridging pap are 6.809 Å in **1**, 6.887 and 7.297 Å in **2**, and 6.936 and 7.250 Å in **3**. Variable-temperature susceptibility measurements on **1**–**3** reveal the occurrence of very weak intramolecular antiferromagnetic interactions between copper(II) ions through bridging pap (the largest value of J being -2.5 cm^{-1}).

Introduction

In recent years much research has been devoted to the syntheses and characterization of one- to three-dimensional polymeric coordination compounds. The supramolecular framework systems that result from utilization of coordination, semi-coordination, hydrogen bonding and the effects of different counter ions in the process of self-assembly are of great interest in the search for materials that may have potential applications related to *e.g.* inclusion phenomena, guest exchange, catalytic properties and molecular-based magnetism.[1] Flexible di- and poly-pyridyl molecules as well as pyrazine have extensively been used as building blocks together with various metal ions for producing supramolecular networks with nanosize pores, and a great variety of topologies have resulted.[1e,2] In many cases, however, interpenetration of lattices occurs, impeding the formation of channels.[3] The pyrazine[2,3-*f*][4,7]phenanthroline (pap) molecule, a heterocyclic, aromatic system with condensed pyrazine and pyridyl rings, has been shown to occur as a rigid, bisbidentate bridge in transition metal complexes,[4] and is expected to be a good building block for creating polynuclear systems where possibly lattice interpenetration is less likely due to the lower flexibility of the ligand.

We have previously reported on dinuclear copper(II)–pap complexes,[4] and in the present contribution focus on higher dimensionality complexes containing the basic pap-bridged copper(II) building block. Three compounds, $[Cu_2(pap)(H_2O)_2(NO_3)_3]_n[NO_3]_n$ **1**, $[Cu_4(pap)_4Cl_7]_nCl_n\cdot 15nH_2O$ **2**, and $[Cu_4(pap)_4(H_2O)_4(C_4O_4)_2]_n[C_4O_4]_n[NO_3]_{2n}\cdot 12nH_2O$ **3**, consisting of alternating, single stranded chains (**1**), chains of chloro-bridged $Cu_4(pap)_4$ units (**2**), and a two-dimensional network of squarate-bridged $Cu_4(pap)_4$ units (**3**), are described (squarate = 3,4-dihydroxy cyclobut-3-ene-1,2-dionate). In the latter two compounds channels, defined by the tetranuclear units, are formed in the crystals. Syntheses, crystal structure determinations and magnetic susceptibility studies have been performed.

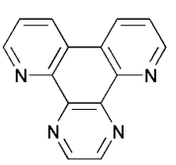

pap

Experimental

Materials

Pyrazino[2,3-*f*][4,7]phenanthroline (pap) was prepared from 4,7-phenanthroline-5,6-dione (a generous gift from Novartis Norge AS) by the procedure of Schmidt and Druey.[5] All other chemicals were purchased from commercial sources and used as received.

Preparations

$[Cu_2(pap)(H_2O)_2(NO_3)_3]_n[NO_3]_n$ 1. 3.9 mmol $Cu(NO_3)_2\cdot 3H_2O$ were added to 1.3 mmol of pap in 20 cm^3 of water and the resulting solution allowed to evaporate nearly to dryness at room temperature. Then, 20 cm^3 of methanol were added. Careful evaporation of the solution yielded green crystals of

DOI: 10.1039/b007983i

Table 1 Summary of crystallographic data and structure refinement for $[Cu_2(pap)(H_2O)_2(NO_3)_3]_n[NO_3]_n$ **1**, $[Cu_4(pap)_4Cl_7]_nCl_n\cdot 15nH_2O$ **2** and $[Cu_4(pap)_4(H_2O)_4(C_4O_4)_2]_n[C_4O_4]_n[NO_3]_{2n}\cdot 12nH_2O$ **3**

	1	**2**	**3**
Formula	$C_{14}H_{12}Cu_2N_8O_{14}$	$C_{56}H_{62}Cl_8Cu_4N_{16}O_{15}$	$C_{68}H_{64}Cu_4N_{18}O_{34}$
M	643.40	1736.98	1931.52
Crystal system	Monoclinic	Monoclinic	Tetragonal
Space group	$P2_1/n$	$P2/n$	$I4_1/amd$
a/Å	10.0172(2)	13.954(2)	24.5977(13)
b/Å	8.85050(10)	12.0954(14)	24.5977(13)
c/Å	24.3125(6)	21.334(3)	25.8003(19)
β/°	95.7700(10)	98.300(2)	90
U/Å^3	2144.56(7)	3563.2(7)	15610.4(16)
Z	4	2	8
μ/mm^{-1}	2.078	1.551	1.179
Reflections collected	18577	15937	36418
Unique reflections	6462 (R_{int} = 0.035)	4376 (R_{int} = 0.126)	3626 (R_{int} = 0.085)
R [$I > 2\sigma(I)$]	0.0377	1.1073	0.0932
R_w [$I > 2\sigma(I)$]	0.0668	0.2690	0.3067

compound **1**. Isopropyl alcohol was added to enhance the precipitation. The crystals were washed with Pr^{i}OH and diethyl ether. The yield was 70% (Found: C, 26.1; H, 1.9; N, 17.3. Calc. for $C_7H_6CuN_4O_7$: C, 26.1; H, 1.9; N, 17.4%).

$[Cu_4(pap)_4Cl_7]_nCl_n\cdot 15nH_2O$ 2. This complex was prepared by adding 0.31 mmol $CuCl_2\cdot 2H_2O$ dissolved in 3 cm^3 of water to 7 cm^3 of a water–EtOH (60 : 40) solution containing 0.31 mmol of pap. Partial evaporation on a hot plate followed by slow cooling afforded thin, light green, diamond-shaped crystals of compound **2**. The yield was 75% (Found: C, 38.5; H, 3.6; N, 13.0. Calc. for $C_{56}H_{62}Cl_8Cu_4N_{16}O_{15}$: C, 38.7; H, 3.6; N, 12.9%).

$[Cu_4(pap)_4(H_2O)_4(C_4O_4)_2]_n[C_4O_4]_n[NO_3]_{2n}\cdot 12nH_2O$ 3. An aqueous solution of lithium squarate (0.14 mmol, 5 cm^3) was slowly added to an aqueous solution containing equimolar amounts of $Cu(NO_3)_2\cdot 3H_2O$ and pap (0.14 mmol each, 15 cm^3) under continuous stirring. Brown micro-crystals of compound **3** precipitated immediately. The yield was 90%. Cube-shaped crystals of **3** suitable for X-ray diffraction work were obtained by slow diffusion in an H-shaped tube with the squarate solution in one arm and the copper(II)–pap solution in the other arm (Found: C, 42.3; H, 3.4; N, 13.0; O, 28.1. Calc. for $C_{34}H_{32}Cu_2N_9O_{17}$: C, 42.3; H, 3.3; N, 13.1; O, 28.2%).

Physical techniques

Infrared spectra were recorded with a Nicolet 800 FTIR spectrophotometer as KBr pellets in the 4000–400 cm^{-1} region. The magnetic susceptibilities of polycrystalline samples were measured over the temperature range 1.8–290 K with a Quantum Design SQUID susceptometer and using an applied magnetic field of 0.1 T. The complex $[NH_4]_2Mn[SO_4]_2\cdot 6H_2O$ was used as a susceptibility standard. Diamagnetic corrections of the constituent atoms were estimated from Pascal's constants and found to be -271×10^{-6} (**1**), -1017×10^{-6} (**2**), and -959×10^{-6} cm^3 mol^{-1} (**3**) per two (**1**) and four (**2** and **3**) copper(II) ions.[6] A value of 60×10^{-6} cm^3 mol^{-1} was used for the temperature-independent paramagnetism of the copper(II) ion.

Crystallography

Crystal parameters and refinement results are summarized in Table 1. Diffraction data were collected using a SMART 2K CCD area detector diffractometer, equipped with an Oxford Cryostream N_2 cooling device.[7] Data for compounds **1** and **3** were collected at 173 K, while for **2** 223 K was used as the crystals cracked on further cooling. The crystals of **2** were thin and extremely fragile and would fracture easily when touched. With care it was, however, possible to mount a crystal in paratone-n oil in a microfibre loop. The data on compound **2** were limited to a $2\theta_{max}$ of 44° due to weak diffraction from the crystal. Empirical absorption corrections were carried out (SADABS).[8] The structures were solved by direct methods and refined by full-matrix least-squares refinement based on F^2 including all reflections. In **1** all non-hydrogen atoms were anisotropically refined. For **2**, due to the data quality and the low fraction of reflections larger than 2σ, isotropic displacement factors were used for all carbon atoms as well as for oxygen atoms in partially occupied positions. In **3** non-hydrogen atoms of the 2-D framework and the squarate counter ion were anisotropically refined, while crystal water oxygen atoms were assigned isotropic thermal parameters. The nitrate counter ion in **3** is located within the cavities of the tetranauclear building blocks, where a cylinder of residual electron density is found. Pronounced disorder did not allow refinement of a reasonable model for this ion, which hence has not been included in the structure factor calculations. For all three structures hydrogen atoms bound to carbon were included at idealized, calculated positions. For compound **1** hydrogens bound to oxygen were located in Fourier difference maps and refined isotropically. In **2** and **3** hydrogens belonging to crystal water could not be located and were not included in the refinements; hydrogen atoms on the coordinated water molecule in **3** were located in a Fourier difference map and refined according to a riding model. In compound **2** part of the water structure is disordered, and after the ordered oxygen atoms had been refined fractional oxygens were fitted to the most dominant residual electron density peaks. Occupancy factors were tentatively refined, and in the final cycles kept fixed at values close to those obtained in the refinement (0.7, 0.5 and 0.3, respectively). The remaining peaks in the difference map were mainly in the open regions of the crystal lattice and are likely due to additional disorder in the water structure. In compound **3** disordered crystal waters were fitted with oxygen atoms of occupancy 0.5.

The SMART and SAINT programs[9] were used for data collections and data integration. Structure solutions, refinements and graphics were performed with the SHELXS 86, SHELXL 93 and XP programs.[10] Selected bond distances and angles are listed in Tables 2–4.

CCDC reference number 186/2297.

See http://www.rsc.org/suppdata/dt/b0/b007983i/ for crystallographic files in .cif format.

Results and discussion

Structures

$[Cu_2(pap)(H_2O)_2(NO_3)_3]_n[NO_3]_n$. The structure consists of single stranded, cationic chains. $[Cu_2(pap)(H_2O)_2(NO_3)_3]_n^{n+}$,

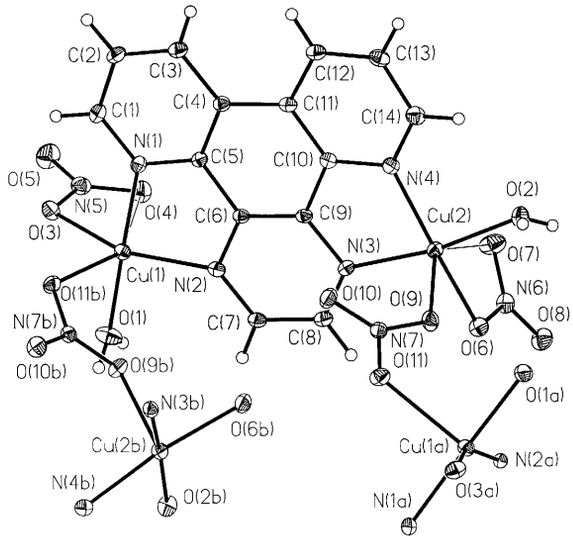

Fig. 1 The building block in the structure of $[Cu_2(pap)(H_2O)_2(NO_3)_3]_n^{n+}$ **1** and its connection to the neighbouring copper sites in the chain. Thermal ellipsoids are plotted at the 30% probability level. Symmetry operations: (a) $-x + 1.5$, $y + 0.5$, $-z + 0.5$; (*b*) $-x + 1.5$, $y - 0.5$, $-z + 0.5$.

Table 2 Selected bond lengths (Å) and angles (°) for $[Cu_2(pap)(H_2O)_2(NO_3)_3]_n[NO_3]_n$ **1**, with e.s.d.s in parentheses

Cu(1)–O(1)	1.943(2)	Cu(2)–O(6)	1.978(2)
Cu(1)–N(1)	2.009(2)	Cu(2)–O(2)	1.984(2)
Cu(1)–O(3)	2.031(2)	Cu(2)–N(4)	2.014(2)
Cu(1)–N(2)	2.039(2)	Cu(2)–N(3)	2.036(2)
Cu(1)–O(11b)	2.239(2)	Cu(2)–O(9)	2.238(2)
Cu(1)···O(4)	2.580(2)	Cu(2)···O(7)	2.524(2)
O(1)–Cu(1)–N(1)	177.82(9)	O(6)–Cu(2)–O(2)	91.50(8)
O(1)–Cu(1)–O(3)	89.15(8)	O(6)–Cu(2)–N(4)	170.38(7)
N(1)–Cu(1)–O(3)	90.48(7)	O(2)–Cu(2)–N(4)	90.47(8)
O(1)–Cu(1)–N(2)	97.11(8)	O(6)–Cu(2)–N(3)	94.24(7)
N(1)–Cu(1)–N(2)	82.38(8)	O(2)–Cu(2)–N(3)	170.14(8)
O(3)–Cu(1)–N(2)	155.85(7)	N(4)–Cu(2)–N(3)	82.58(8)
O(1)–Cu(1)–O(11b)	89.88(8)	O(6)–Cu(2)–O(9)	81.92(7)
N(1)–Cu(1)–O(11b)	92.29(7)	O(2)–Cu(2)–O(9)	88.06(7)
O(3)–Cu(1)–O(11b)	93.89(7)	N(4)–Cu(2)–O(9)	107.56(7)
N(2)–Cu(1)–O(11b)	109.36(7)	N(3)–Cu(2)–O(9)	100.67(7)
O(1)–Cu(1)–O(4)	90.76(8)	O(6)–Cu(2)–O(7)	56.10(6)
N(1)–Cu(1)–O(4)	87.28(7)	O(2)–Cu(2)–O(7)	84.58(8)
O(3)–Cu(1)–O(4)	54.77(6)	N(4)–Cu(2)–O(7)	114.77(7)
N(2)–Cu(1)–O(4)	101.67(7)	N(3)–Cu(2)–O(7)	91.98(7)
O(11b)–Cu(1)–O(4)	148.64(6)	O(9)–Cu(2)–O(7)	137.03(6)

Symmetry transformation used to generate equivalent atoms: (b) $-x + 1.5$, $y - 0.5$, $-z + 0.5$.

and uncoordinated nitrate counter ions. The pap and nitrate groups alternate as bridges between copper atoms, the chain extending along a twofold screw axis in zigzag fashion where the Cu(1)–Cu(2)–Cu(1a) and Cu(2)–Cu(1)–Cu(2b) angles are 110.1(1) and 68.8(1)°, respectively (Fig. 1). Neighbouring chains are firmly linked through hydrogen bonds between coordinated nitrate and coordinated water molecules. The counter ion serves to reinforce this through hydrogen bonds to coordinated water in two different chains. The packing arrangement is rather compact, as revealed by the high density of this compound, considering the Cu : (C,N,O) ratio.

The coordination geometries of the two independent copper atoms may to a first approximation be described as distorted square pyramidal. In each case two pap nitrogen atoms (Cu–N 2.009(2)–2.039(2) Å), a water and a nitrate oxygen atom (Cu–O 1.943(2)–2.031(2) Å) constitute the equatorial plane, and an oxygen of the bridging nitrate occupies the apical position (Cu–O 2.238(2)–2.239(2) Å). The configurations of the two coordination spheres differ, however, as the *trans* position to the

Table 3 Selected bond lengths (Å) and angles (°) for $[Cu_4(pap)_4Cl_7]_nCl_n \cdot 15nH_2O$ with e.s.d.s in parentheses

Cu(1)–N(1)	2.000(13)	Cu(2)–N(4a)	2.018(15)
Cu(1)–N(5)	2.041(14)	Cu(2)–N(8)	2.024(15)
Cu(1)–N(2)	2.086(14)	Cu(2)–N(3a)	2.077(12)
Cu(1)–Cl(1)	2.264(6)	Cu(2)–Cl(3)	2.271(5)
Cu(1)–N(6)	2.314(14)	Cu(2)–N(7)	2.311(15)
Cu(1)–Cl(2)	2.734(4)	Cu(2)–Cl(4)	2.64(2)
N(1)–Cu(1)–N(5)	166.7(6)	N(4a)–Cu(2)–N(8)	168.5(6)
N(1)–Cu(1)–N(2)	80.8(5)	N(4a)–Cu(2)–N(3a)	80.2(5)
N(5)–Cu(1)–N(2)	90.0(5)	N(8)–Cu(2)–N(3a)	92.3(5)
N(1)–Cu(1)–Cl(1)	96.5(4)	N(4a)–Cu(2)–Cl(3)	95.1(4)
N(5)–Cu(1)–Cl(1)	93.2(4)	N(8)–Cu(2)–Cl(3)	93.9(4)
N(2)–Cu(1)–Cl(1)	175.5(4)	N(3a)–Cu(2)–Cl(3)	168.0(4)
N(1)–Cu(1)–N(6)	93.6(5)	N(4a)–Cu(2)–N(7)	93.2(5)
N(5)–Cu(1)–N(6)	76.3(5)	N(8)–Cu(2)–N(7)	77.9(5)
N(2)–Cu(1)–N(6)	87.9(5)	N(3a)–Cu(2)–N(7)	88.4(5)
Cl(1)–Cu(1)–N(6)	95.9(4)	Cl(3)–Cu(2)–N(7)	102.9(4)
N(1)–Cu(1)–Cl(2)	92.9(4)	N(4a)–Cu(2)–Cl(4)	96.4(5)
N(5)–Cu(1)–Cl(2)	95.6(5)	N(8)–Cu(2)–Cl(4)	90.4(5)
N(2)–Cu(1)–Cl(2)	83.2(4)	N(3a)–Cu(2)–Cl(4)	78.0(5)
Cl(1)–Cu(1)–Cl(2)	93.4(2)	Cl(3)–Cu(2)–Cl(4)	91.7(3)
N(6)–Cu(1)–Cl(2)	168.0(4)	N(7)–Cu(2)–Cl(4)	161.8(4)
Cu(1)–Cl(2)–Cu(1b)	138.4(3)		

Symmetry transformations used to generate equivalent atoms: (a) $-x + 1.5$, y, $-z + 0.5$; (b) $-x + 0.5$, y, $-z + 0.5$.

equatorial water in one case (Cu(1)) is occupied by a pyridyl nitrogen and in the other case (Cu(2)) by a pyrazine nitrogen atom. Each non-bridging coordinated nitrate makes an additional semi-coordinated bond to copper (Cu···O 2.580(2) and 2.524(2) Å), hence the copper coordination may also be considered strongly distorted octahedral 4 + 1 + 1*.[11] The pap bridge is essentially planar and makes angles of 11.27(8) and 8.70(8)° with the Cu(1) and Cu(2) equatorial planes. The intrachain copper–copper separations are 6.809(1) and 5.194(1) Å across the pap and nitrato bridges, respectively. The shortest interchain copper–copper distance is 5.576(1) Å.

We have previously reported on a dinuclear copper(II) complex of formula $[Cu_2(pap)(H_2O)_3(NO_3)_3]NO_3$ **4**,[4] which in composition differs from **1** only in having one more coordinated water molecule. The two compounds crystallize in the same space group and their crystal structures show some striking similarities. A twist of the axially coordinated nitrate in the dinuclear compound together with a relatively small molecular displacement will allow an axial O,O′-nitrate bridge to be formed between copper atoms, resulting in an alternating chain. In synthesizing these compounds, the dinuclear complex crystallises from an aqueous solution after evaporation,[4] whereas **1** crystallises if an alcohol is added to the aqueous solution just before precipitation starts.

$[Cu_4(pap)_4Cl_7]_nCl_n \cdot 15nH_2O$ 2. The cyclic, tetranuclear entity (Fig. 2) with four copper atoms bridged by bisbidentate pap ligands is made up of two asymmetric units related by a twofold axis, and constitutes the basic structural building block in this compound. One of the chlorine atoms (Cl(2)) serves as a mono(μ-chloro) bridge between such units, generating chains (Fig. 3) which extend along the crystallographic *a* axis. The crystal packing results in partial overlap between parallel pap groups in neighbouring chains, the average interplanar distance between pap2 (N(5) through N(8), C(21) through C(34)) and pap2 ($1 - x$, $-y$, $-z$) being 3.42(2) Å. Along the *b*-axis chains stack on top of each other one unit cell apart so that the square voids, defined by the tetranuclear entities, together form channels running parallel to *b*. One of the ordered water molecules apparently form hydrogen bonds to coordinated chlorine atoms in two consecutive tetranuclear units within a chain, and thus serves to stabilize the chain structure. Only weak forces due to stacking interactions and Cl···H–C and

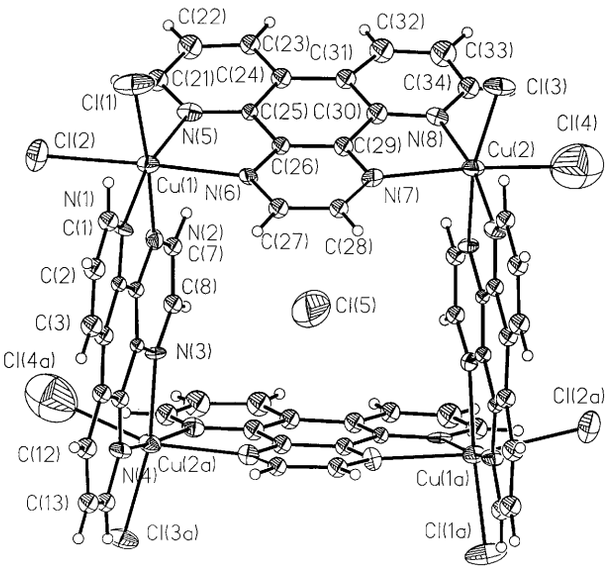

Fig. 2 The tetranuclear entity in $[Cu_4(pap)_4Cl_7]_nCl_n \cdot 15nH_2O$ **2**. Thermal ellipsoids are plotted at the 30% probability level. Symmetry operation: (a) $-x + 1.5, y, -z + 0.5$.

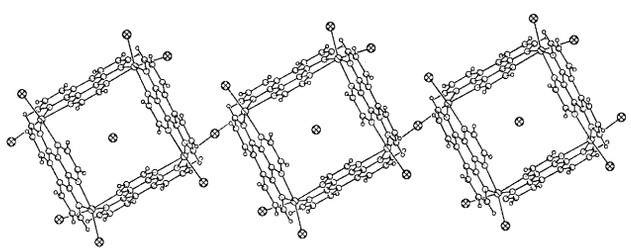

Fig. 3 Section of chain of chloro-bridged tetranuclear entities in compound **2**.

$H_2O \cdots H$–C contacts serve to tie neighbour chains together, and this accounts for the extreme fragility of the crystals. The chloride counter ion is situated on the twofold axis in the middle of the cavity of the tetranuclear unit (Fig. 2). Its position appears to be stabilized through hydrogen bonds to water of hydration ($Cl \cdots O$ 3.21(4) and 3.02(4) Å) and through weak interactions with pap, an aromatic π acceptor, the distances from Cl(5) to the planes of the two pap ligands being 3.53(8) and 3.41(7) Å, respectively. Attraction between chlorine and the π-electron systems of heterocycles has previously been discussed.[12a,b]

The two crystallographically independent copper atoms both have elongated octahedral geometries. In each case one chlorine, one pyrazine nitrogen and two pyridyl nitrogen atoms constitute the equatorial plane, while one chlorine and one pyrazine nitrogen atom coordinate in the axial positions. The lengths of the axial Cu–Cl bonds (2.734(4) and 2.638(16) Å) are in agreement with those found for bridging, axial Cl in $[Cu_2(bpym)(ox)Cl_2]_n$ (2.557(1) and 2.828(1) Å)[12c] and in $[Cu(bipy)Cl_2]$ (2.674(3) Å)[12d] (bpym = 2,2′-bipoyrimide, bipy = 2,2′-bipyridine, ox = oxalate). The equatorial Cu–Cl bond lengths (2.264(6)–2.314(14) Å) are comparable to those found in the sheetlike $[Cu_2(bpym)Cl_4]$,[12e] the chain $[Cu(bipy)Cl_2]$,[12d] and the dinuclear $[Cu_2(dpp)(dmso)(H_2O)Cl_4] \cdot dmso$[12f] complexes (dpp = 2,3-di-2-pyridylpyrazine and dmso = dimethyl sulfoxide). The two crystallographically independent pap ligands bridge the metal atoms differently; while the plane of pap1 (N(1) through N(4), C(1) through C(14)) is almost coplanar with the copper equatorial planes (dihedral angles 5.7(4) and 9.5(4)° with respect to Cu(1) and Cu(2a) equatorial planes), that of pap2 (N(5) through N(8), C(21) through C(30)) is close to perpendicular to the equatorial planes of Cu(1) and Cu(2) (dihedral angles 83.7(2) and 80.9(2)°, respectively), Fig. 2.

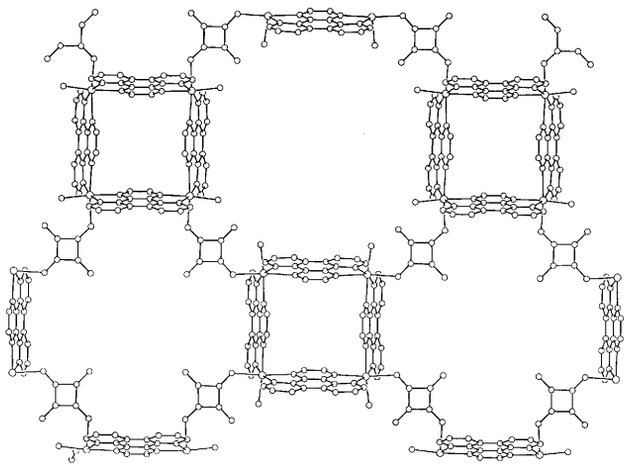

Fig. 4 Sheet structure of compound **3**, $[Cu_4(pap)_4(H_2O)_4(C_4O_4)_2]_n$-$[C_4O_4]_n[NO_3]_{2n} \cdot 12nH_2O$.

The bond angle at the chlorine forming the bridge between tetranuclear units, Cu(1)–Cl(2)–Cu(1b), is 138.4(4)° [(b) $0.5 - x, y, 0.5 - z$].

The copper–copper separation across the equatorially coordinated pap ligand is somewhat shorter ($Cu(1) \cdots Cu(2a)$ 6.887(3) Å) than that across the pap bridge which is oriented close to normal to the metal equatorial planes ($Cu(1) \cdots Cu(2)$ 7.297(3) Å). The diagonal copper–copper distances within the tetranuclear unit are 10.082(4) and 9.978(5) Å for $Cu(1) \cdots Cu(1a)$ and $Cu(2) \cdots Cu(2a)$, respectively. The shortest intrachain copper−copper separation occurs across the axial chlorine bridge ($Cu(1) \cdots Cu(1b)$ 5.110(5) Å), whereas the shortest interchain copper–copper distance is much longer [$Cu(1) \cdots Cu(2c)$ 7.489(3) Å; (c) $1 - x, 1 - y, -z$].

$[Cu_4(pap)_4(H_2O)_4(C_4O_4)_2]_n[C_4O_4]_n[NO_3]_{2n} \cdot 12nH_2O$. This structure also has a cyclic, tetranuclear building block with copper atoms bridged by pap ligands. In this case, however, coordinated squarate, exhibiting a μ-1,3 bridging mode, links these building blocks into sheets creating two types of void space between the tetranuclear entities, each bordered by eight metal ions, four pap groups and four squarate groups (Fig. 4). Hydrogen bonds between bridging squarate and the coordinated water molecules provide additional stabilization to this open framework ($O(1) \cdots O(3)$ 2.650(6) Å). In the crystals the sheets stack so that the $Cu_4(pap)_4$ entities of one sheet overlap and protrude partly into the voids in the neighbouring sheets (Fig. 5). Uncoordinated squarate counter ions link the sheets by rather strong hydrogen bonds to coordinated water molecules ($O(1) \cdots O(5) = 2.626(8)$ Å). The structure displays channels running normal to the sheets and through the tetranuclear entities. The disordered nitrate counter ion is housed within the cavity of the tetranuclear building block, while disordered water molecules are found between sheets, mainly in the channels.

The copper(II) coordination is elongated octahedral with one water oxygen, one pyrazine nitrogen and two pyridyl nitrogen atoms in the equatorial plane, and one squarate oxygen and one pyrazine nitrogen atom in axial positions. Although the point symmetry of the tetranuclear building block in compound **3** is higher (*2mm*) than in **2** (2), the geometries of the units are very similar. Also in **3** there are two different pap bridges within the tetranuclear unit; one bridging copper through equatorial coordination only, while the other binds equatorially to copper through pyridyl nitrogen atoms and in axial positions through pyrazine nitrogen atoms. The pap ligand binding in equatorial positions only is almost coplanar with the copper equitorial plane (dihedral angle 6.8(2)°), while pap binding in equatorial and axial positions is close to normal to the equatorial plane (dihedral angle 85.5(1)°).

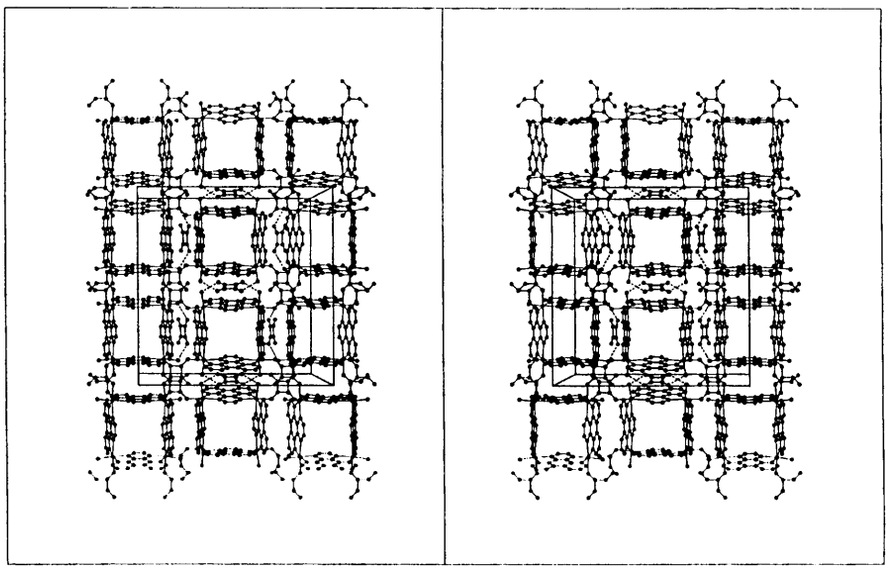

Fig. 5 Crystal packing in compound **3**, $[Cu_4(pap)_4(H_2O)_4(C_4O_4)_2]_n[C_4O_4]_n[NO_3]_{2n}\cdot 12nH_2O$.

Table 4 Selected bond lengths (Å) and bond angles (°) for $[Cu_4(pap)_4(H_2O)_4(C_4O_4)_2]_n[C_4O_4]_n[NO_3]_{2n}\cdot 12nH_2O$ **3** with e.s.d.s in parentheses

Cu(1)–N(4)	2.011(6)	Cu(1)–N(3)	2.118(6)
Cu(1)–N(1)	2.032(7)	Cu(1)–O(2)	2.242(7)
Cu(1)–O(1)	2.040(6)	Cu(1)–N(2)	2.278(7)
N(4)–Cu(1)–N(1)	168.2(3)	O(1)–Cu(1)–O(2)	91.4(2)
N(4)–Cu(1)–O(1)	92.8(2)	N(3)–Cu(1)–O(2)	85.2(2)
N(1)–Cu(1)–O(1)	94.1(2)	N(4)–Cu(1)–N(2)	92.0(2)
N(4)–Cu(1)–N(3)	80.7(2)	N(1)–Cu(1)–N(2)	77.8(3)
N(1)–Cu(1)–N(3)	92.9(3)	O(1)–Cu(1)–N(2)	95.5(2)
O(1)–Cu(1)–N(3)	172.6(2)	N(3)–Cu(1)–N(2)	88.3(2)
N(4)–Cu(1)–O(2)	90.7(2)	O(2)–Cu(1)–N(2)	172.4(2)
N(1)–Cu(1)–O(2)	98.6(3)	C(22)–O(2)–Cu(1)	129.4(6)

The coordinated squarate adopts a μ-1,3-bismonodentate binding mode, bridging copper atoms in two neighbouring tetranuclear units. It has previously been documented that squarate binds to 3d metal ions both in monodentate, bismonodentate (μ-1,2 and μ-1,3 bridges) and tetramonodentate (μ-1,2,3,4 bridge) coordination modes,[13] while chelating and bischelating modes are not found due to the large bite distance of this ligand.[14] The coordinated and free squarate groups are planar and their bond lengths and angles in agreement with those observed in previous structures of squarate-containing copper(II) complexes.

The copper–copper distance across the all equatorially coordinated pap (6.936(2) Å) is somewhat shorter than that observed across the other pap bridge (7.250(2) Å); the metal–metal separation along the diagonal is 10.034(2) Å. Within each sheet the *exo*-tetranuclear copper–copper distance across the bridging squarate is 7.576(2) Å. The shortest *exo*-tetranuclear copper–copper separation, however, occurs across the squarate counter ion (7.106(2) Å) which forms hydrogen bonded links between neighbour sheets. In the crystal lattice pap groups and squarate counter ion stack almost parallel and with partial overlap. The distances from the overlapping atoms of the uncoordinated squarate to the mean plane of the equatorially/axially coordinated pap are relatively short, ranging from 3.23 to 3.34 Å, the dihedral angle between the pap and squarate planes being 6.7(2)°. The equatorially/axially coordinated pap of one layer also partially overlaps an all equatorially coordinated pap in the neighbouring sheet, the atomic distances in the overlapping part ranging from 3.41 to 3.47 Å, and the dihedral angles between the planes being 1.3(1)°.

A variety of tetranuclear parallelogram or square copper(II) complexes with bridging organic ligands have been described.[15] Assemblies of such units in the form of ladders and two-dimensional grids with the squares as repetition units have also been synthesized, especially based on 4,4′-bipyridine as bridging ligand.[2,3c,16] In the present case with pap as bridging ligand within the square units the modes of linking differ from those observed with bipyridine bridges; in **2** linking of squares through diagonally opposite corners occur by a chloro ligand into chains, and in **3** linking of the squares through all corners by squarato ligands into a two-dimensional network where the squares alternate with two different types of rings containing eight metal ions, four pap and four squarate bridges.

Infrared spectra

Free pap shows a number of strong to medium absorption bands in the 1650 to 1300 cm^{-1} region; 1647 (br) s, 1590 s, 1527 m, 1481 s, 1419 s and 1392 s cm^{-1}.[4] Wide portions of this region are obscured in the spectra of complexes **1** and **3** due to the occurrence of strong absorptions for nitrate and squarate, while in the spectrum of **2** one can observe a pattern which is similar to that of free pap, only marginally affected by the metal complexation. The presence of nitrate in **1** is evidenced by a broad feature centered around 1390 cm^{-1} and peaks at 825, 807 and 725 cm^{-1} as well as the combination band at 1760 cm^{-1}.[17] The spectrum of **3** is dominated by a strong and broad band centred at around 1500 cm^{-1}, characteristic of squarate salts, and attributed to vibrational modes representing mixtures of C–O and C–C stretching motions.[18]

Magnetic properties

The magnetic properties of complex **1** in the form of $\chi_m T$ *versus* T and χ_m *versus* T plots (χ_m being the magnetic susceptibility per two copper(II) ions) have been recorded. $\chi_m T$ at room temperature is equal to 0.83 cm^3 K mol^{-1}, a value expected for two magnetically isolated spin doublets. It remains practically constant when cooling and decreases sharply at $T < 20$ K reaching a value of 0.43 cm^3 K mol^{-1} at 1.8 K. An incipient maximum of susceptibility is observed at 1.8 K in the χ_m *versus* T curve. These results are typical of a quasi Curie law magnetic behaviour with a very weak antiferromagnetic interaction. Although the crystal structure of **1** corresponds to an alternating chain with regular alternation of pap and nitrato bridges, the fact that the dinuclear pap-bridged copper(II) units are linked through long axial Cu–O(nitrato) bonds prompted us to analyse its magnetic behaviour through a simple Bleaney–Bowers expression[19] with the Hamiltonian $\hat{H} = -J\,\hat{S}_1\cdot\hat{S}_2$ (J is the singlet–triplet energy gap). The values of the magnetic

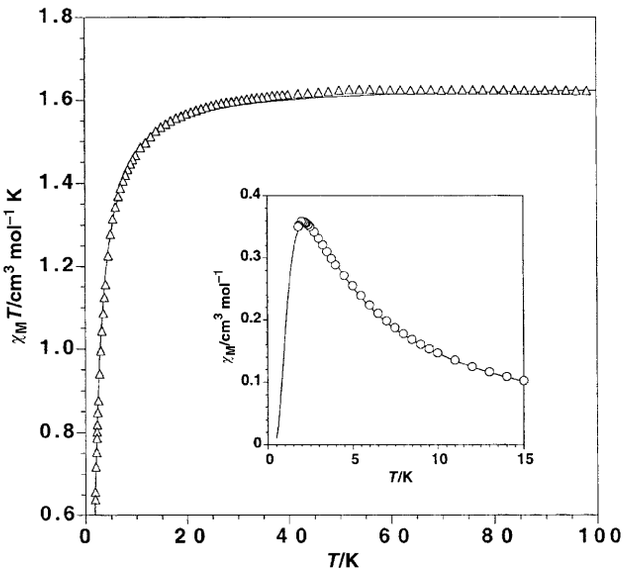

Fig. 6 Thermal dependence of χT (△) for complex **2**; the solid line is the best fit (see text). The insert shows the susceptibility curve (○) in the low temperature region.

parameters obtained by least-squares fit through this Hamiltonian are: $J = -2.0$ cm^{-1}, $g = 2.11$ and $R = 1.6 \times 10^{-5}$ (R is the agreement factor defined as $\Sigma_i [(\chi_m T)_{obs(i)} - (\chi_m T)_{calc(i)}]^2/\Sigma_i [(\chi_m T)_{obs(i)}]^2$). The analysis of the magnetic properties of **1** through the appropriate Hamiltonian for an alternating chain [$\hat{H} = -J \Sigma_i(\hat{S}_{i-1}\cdot\hat{S}_i + a\hat{S}_i\cdot\hat{S}_{i+1})$][20] (where a is the alternating parameter) gave a value of a of practically zero and those of J and g the same as in the preceding fit. So, the simpler dinuclear model for **1** seems correct. This is not surprising as the magnetic orbital on each copper atom is clearly of the d($x^2 - y^2$) type and oriented in the plane of the pap bridge. The most efficient exchange pathway is thus assumed to be through the bridging pap (σ in-plane exchange pathway), while the magnetic coupling through the nitrate bridge (axial exchange pathway) is expected to be negligible due to the very weak overlap between the magnetic orbitals *via* the longer axial bonds. The small value of the antiferromagnetic coupling in **1** is in agreement with those recently reported through equatorially coordinated pap for dinuclear pap-bridged copper(II) complexes (J values in the range -1.3 to -1.6 cm^{-1})[4] with similar CuN_2O_4 coordination spheres being involved.

The magnetic properties of complexes **2** and **3** are very similar; the magnetic curve of **2** in the form of a $\chi_m T$ *versus* T plot (χ being the magnetic susceptibility per four copper(II) ions) is shown in Fig. 6. The values of $\chi_m T$ at room temperature for **2** and **3** are 1.63 and 1.61 cm^3 K mol^{-1}, respectively, as expected for four magnetically isolated spin doublets. These values remain constant when cooling and only exhibit a significant decrease in the low temperature region [0.13 (**2**) and 0.26 cm^3 K mol^{-1} (**3**) at 1.8 K]. A maximum in the susceptibility curve is observed at 2.1 K for complex **2** (see insert of Fig. 6) whereas no maximum occurs in the corresponding susceptibility curve of **3**. These features in the magnetic curves are characteristic of the occurrence of very weak antiferromagnetic interaction between the copper(II) ions. Looking at the structures of **2** and **3**, one can see that the magnetic orbital on each copper(II) ion is located in the best equatorial plane involving the four short ligand to metal distances: N(1)N(2)N(5)Cl(1) and N(3a)N(4a)N(8)Cl(3) at Cu(1) and Cu(2), respectively, in complex **2**; O(1)N(1)N(3)N(4) at Cu(1) in **3**. The most efficient exchange pathway hence most likely involves the pap bridging ligands. As one pair of pap bridges are all equatorially coordinated while another pair of such bridges are coordinated axially and equatorially, two different exchange coupling parameters (J_1 and J_2) between pairs of copper(II) ions within the tetranuclear unit will have to be considered as indicated in Scheme 1.

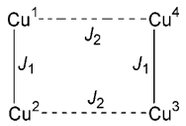

Scheme 1

The corresponding Hamiltonian is given by eqn. (1) where

$$\hat{H} = -J_1[\hat{S}_1\cdot\hat{S}_2 + \hat{S}_3\cdot\hat{S}_4] - J_2[\hat{S}_2\cdot\hat{S}_3 + \hat{S}_1\cdot\hat{S}_4] \qquad (1)$$

$S_1 = S_2 = S_3 = S_4 = \frac{1}{2}$ (local spins). There is no solution for this system through the vector coupling model,[21] and to treat the magnetic data we used numerical matrix diagonalization techniques.[22,23] A least-squares fit leads to the following set of parameters: $J_1 = -2.5$ cm^{-1}, $J_1 = -0.2$ cm^{-1}, $g = 2.09$ and $R = 2.6 \times 10^{-4}$ for **2** and $J_1 = -2.1$ cm^{-1}, $J_2 = -0.1$ cm^{-1}, $g = 2.09$ and $R = 3.4 \times 10^{-4}$ for **3**. The calculated curves match well the magnetic data in both cases.

The values of J_1, -2.5 for compound **2** and -2.1 cm^{-1} for **3**, are comparable to the exchange parameter found for **1**, and must be assumed to reflect the exchange through the pap ligand which is approximately coplanar with the copper equatorial plane, and where the Cu···Cu separations are 6.887 (**2**) and 6.936 Å (**3**); while J_2 (-0.2 (**2**) and -0.1 cm^{-1} (**3**)) may be referred to the other pap ligand where pyrazine is axially coordinated to copper, resulting in larger Cu···Cu separations of 7.297 (**2**) and 7.250 Å (**3**). The differences in the J_1 values of compounds **1**–**3**, although small, may be related to the differences in the sets of donor atoms in the compounds. Previous studies have shown that the less electronegative the peripheral donor atoms, and the more diffuse their valence electron densities are, the greater is the spin delocalization onto the bridge, and the larger is the magnetic coupling.[24] The trend observed in **1**–**3** fits into this scheme; in **1** the copper coordination sphere is defined by an N_2O_4 set of atoms (magnetic orbitals defined by N_2O_2), while in **2** and **3** N_4Cl_2 and N_4O_2, respectively, constitute the surroundings (magnetic orbitals defined by N_3Cl and N_3O).

In the magnetic analysis of complexes **2** and **3** we have neglected the exchange pathway through single-chloro (**2**) and μ-1,3-squarato (**3**) bridges. Concerning the former possibility, one must keep in mind that the exchange pathway would involve the Cu(1)–Cl(2)–Cu(1b) unit where both metal to chloro bonds are weak axial interactions (2.734(4) Å). The overlap between the magnetic orbitals through this weak axial pathway must be extremely small and consequently the magnetic coupling must be negligible. As far as the squarato bridge is concerned, it has been demonstrated in previous magneto-structural studies that the exchange between copper(II) ions through a μ-1,3-squarate bridge is small even when the copper to squarate oxygen (bridge) bonds are short, equatorial bonds.[13a,b,14] In the present case, with axial copper to squarate oxygen bonds, the overlap between the magnetic orbitals must be negligible and, consequently, the magnetic interaction through the squarate in **3** is assumed to be zero.

Summarizing, in the present contribution we show how the use of rigid pap as bridging ligand in the presence of coordinating anions such as nitrate (**1**), chloride (**2**) and squarate (**3**) allowed us to prepare either an alternating copper(II) chain where the dinuclear Cu_2(pap) units are connected through bis-monodentate nitrato bridges (**1**), or unprecedented Cu_4(pap)$_4$ tetrauclear entities linked by single-chloro (**2**) or μ-1,3-squarato (**3**) bridges affording one-dimensional (**2**) and two-dimensional sheet-like (**3**) polymers. In **1** and **2** the tetranuclear units define the cross sections of channels running through the crystal

lattice. The magnetic coupling between copper(II) ions through bridging pap (copper–copper separation 6.8 Å or larger) is weak and antiferromagnetic in nature.

Acknowledgements

The gift of 4,7-phenanthroline-5,6-dione from Novartis Norge AS is greatly appreciated. Grants from NFR (Research Council of Norway) and the University of Bergen allowing the purchase of X-ray equipment, a Ph.D.-student fellowship (H. G.) from the University of Bergen, as well as partial financial support (M. J. and F. L.) from the Spanish Dirección General de Investigación Científica y Técnica through project PB97–1397 is acknowledged. Thanks are also extended to the Centre d'Informàtica of the University of Valencia for computer resource support.

References

1 (*a*) P. J. Stang and B. Olenyuk, *Acc. Chem. Res.*, 1997, **30**, 502; (*b*) C. Janiak, *Angew. Chem., Int. Ed. Engl.*, 1997, **36**, 1431; (*c*) C. L. Bowes and G. A. Ozin, *Adv. Mater.*, 1996, **8**, 13; (*d*) *Magnetic Molecular Materials*, eds. D. Gatteschi, O. Kahn, J. S. Miller and F. Palacio, Kluwer Academic Publishers, Dordrecht, 1991; (*e*) J.-M. Lehn, *Supramolecular Chemistry – Concepts and Perspectives*, VCH Verlagsgesellschaft, Weinheim, 1995 and references therein.

2 B. Olenyuk, A. Fechtenkötter and P. Stang, *J. Chem. Soc., Dalton Trans.*, 1998, 1707.

3 (*a*) S. S.-Y. Chui, S. M.-F. Lo, J. P. H. Charmant, A. G. Orpen and I. D. Williams, *Science*, 1999, **283**, 1148; (*b*) S. R. Batten and R. Robson, *Angew. Chem., Int. Ed.*, 1998, **37**, 1460; (*c*) P. Losier and M. J. Zaworotko, *Angew. Chem., Int. Ed. Engl.*, 1996, **35**, 2779, and references therein.

4 H. Grove, J. Sletten, M. Julve and F. Lloret, *J. Chem. Soc., Dalton Trans.*, 2000, 515.

5 P. Schmidt and J. Druey, *Helv. Chim. Acta*, 1957, **40**, 350; S. Imor, R. J. Morgan, S. Wang, O. Morgan and A. D. Baker, *Synth. Commun.*, 1996, **26**, 2197.

6 A. Earnshaw, in *Introduction to Magnetochemistry*, Academic Press, London, 1968.

7 J. Cosier and F. H. Glazer, *J. Appl. Crystallogr.*, 1986, **19**, 105.

8 G. M. Sheldrick, SADABS, Empirical Absorption Correction Program, University of Göttingen, 1996.

9 SMART, Version 4.0, Data Collection Software and SAINT, Version 4.0, Data Integration Software, Bruker AXS, Inc., Madison, WI, 1997.

10 G. M. Sheldrick, *Acta Crystallogr., Sect. A*, 1990, **46**, 467; G. M. Sheldrick, SHELXL 93, University of Göttingen, 1993, XP, Version 4.3, Siemens Analytical X-ray Inst. Inc., Madison, WI, 1992.

11 I. M. Procter, B. J. Hathaway and P. Nicholls, *J. Chem. Soc. A*, 1968, 1678; B. J. Hathaway, *Struct. Bonding* (*Berlin*), 1984, **57**, 55.

12 (*a*) J. A. Carrabine and M. Sundaralingam, *J. Am. Chem. Soc.*, 1970, **92**, 369; (*b*) E. Sletten, J. Sletten and N. Å. Frøystein, *Acta Chem. Scand., Ser. A*, 1988, **42**, 413; (*c*) S. Decurtins, H. W. Schmalle, P. Schneuwly, L.-M. Zheng, J. Ensling and A. Hauser, *Inorg. Chem.*, 1995, **34**, 5501; (*d*) M. Hernández-Molina, J. González-Platas, C. Ruiz-Pérez, F. Loret and M. Julve, *Inorg. Chim. Acta*, 1999, **284**, 258; (*e*) M. Julve, G. De Munno, G. Bruno and M. Verdaguer, *Inorg. Chem.*, 1988, **27**, 3160; (*f*) H. Grove and J. Sletten, unpublished work.

13 (*a*) I. Castro, J. Faus, M. Julve, Y. Journaux and J. Sletten, *J. Chem. Soc., Dalton Trans.*, 1991, 2533; (*b*) I. Castro, J. Sletten, M. L. Calatayud, M. Julve, J. Cano, F. Lloret and A. Caneschi, *Inorg. Chem.*, 1995, **34**, 4903; (*c*) I. Castro, M. L. Calatayud, J. Sletten, F. Lloret and M. Julve, *J. Chem. Soc., Dalton Trans.*, 1997, 811; (*d*) I. Castro, M. L. Calatayud, J. Sletten, F. Lloret and M. Julve, *Inorg. Chim. Acta*, 1999, **287**, 173.

14 X. Solans, M. Aguiló, A. Gleizes, J. Faus, M. Julve and M. Verdaguer, *Inorg. Chem.*, 1990, **29**, 775.

15 K. S. Murray, *Adv. Inorg. Chem.*, 1995, **43**, 261; E. Colacio, C. López-Magaña, V. McKee and A. Romerosa, *J. Chem. Soc., Dalton Trans.*, 1999, 2923.

16 J. Li, H. Zeng, J. Chen, Q. Wang and X. Wu, *Chem. Commun.*, 1997, 1213; M. Fujita, Y. J. Kwon, S. Washizu and K. Ogura, *J. Am. Chem. Soc.*, 1994, **116**, 1151 and references therein.

17 C. C. Addison, N. Logan, S. C. Wallwork and C. D. Garner, *Q. Rev. Chem. Soc.*, 1971, **25**, 289; K. Nakamoto, in *Infrared and Raman Spectra of Inorganic and Coordination Compounds*, 3rd edn., John Wiley & Sons, New York, 1978.

18 M. Ito and R. West, *J. Am. Chem. Soc.*, 1963, **85**, 2580.

19 B. Bleaney and K. D. Bowers, *Proc. R. Soc. London, Ser. A*, 1952, **214**, 451.

20 W. Duffy and K. P. Barr, *Phys. Rev.*, 1968, **165**, 647; J. W. Hall, W. E. Marsh, R. R. Welles and W. E. Hatfield, *Inorg. Chem.*, 1981, **20**, 1033.

21 K. Kambe, *Phys. Soc. Jpn.*, 1950, **5**, 48.

22 K. J. Berry, P. E. Clark, K. A. Murray, C. L. Raston and A. H. White, *Inorg. Chem.*, 1983, **22**, 3920.

23 The quantity of $\chi_m T$ is related to the fluctuation of the magnetization M, which is calculated from the energy eigenvalues and spin eigenfunctions. The eigensystem solution has been achieved by diagonalizing the energy matrix. For the tetranuclear $Cu_4(pap)_4$ units of compounds **2** and **3** the number of microstates is given by $(2S_{Cu} + 1)^4 = 16$. However, the matrices are built from the spin function basis in the M_S sub-spaces, where M_S is the z component of the spin quantum number S. In this case, the size of the largest matrix that must be diagonalized corresponds to the $M_S = 0$ sub-space and is 6×6.

24 P. Román, C. Guzmán-Miralles, A. Luque, J. I. Beitia, J. Cano, F. Lloret, M. Julve and S. Alvarez, *Inorg. Chem.*, 1996, **35**, 3741.